

A HIGH-ENTROPY WIND R-PROCESS STUDY BASED ON NUCLEAR-STRUCTURE QUANTITIES FROM THE NEW FINITE-RANGE DROPLET MODEL FRDM(2012)

KARL-LUDWIG KRATZ^{1,2}, KHALIL FAROUQI^{3,4}, AND PETER MÖLLER⁵

¹Max-Planck-Institut für Chemie (Otto-Hahn-Institut), D-55128 Mainz, Germany;klk@uni-mainz.de

²Fachbereich Chemie, Pharmazie und Geowissenschaften, Universität Mainz, D-55128 Mainz, Germany

³Zentrum für Astronomie der Universität Heidelberg, Landessternwarte, D-69117 Heidelberg, Germany;kfarouqi@lsw.uni-heidelberg.de

⁴Department of Physics, University of Basel, Klingelbergstrasse 82, CH-4056 Basel, Switzerland and

⁵Theoretical Division MS B214, Los Alamos National Laboratory, Los Alamos, NM 87545, USA;moller@lanl.gov

ACCEPTED FOR PUBLICATION IN THE ASTROPHYSICAL JOURNAL

ABSTRACT

Theoretical studies of the nucleosynthesis origin of the heavy elements in our Solar System (S.S.) by the rapid neutron-capture process (r-process) still face the entwined uncertainties in the possible astrophysical scenarios and the nuclear-physics properties far from stability. In this paper we present results from the investigation of an r-process in the high-entropy wind (HEW) of core-collapse supernovae (here chosen as one of the possible scenarios for this nucleosynthesis process), using new nuclear-data input calculated in a consistent approach, for masses and β -decay properties from the new finite-range droplet model FRDM(2012). The accuracy of the new mass model is 0.56 MeV with respect to AME2003, to which it was adjusted. We compare the new HEW r-process abundance pattern to the latest S.S. r-process residuals and to our earlier calculations with the nuclear-structure quantities based on FRDM(1992). Substantial overall and specific local improvements in the calculated pattern of the r-process between $A \simeq 110$ and ^{209}Bi , as well as remaining deficiencies are discussed in terms of the underlying spherical and deformed shell structure far from stability.

Keywords: nuclear reactions, nucleosynthesis, abundances

1. INTRODUCTION

Among the most challenging tasks in nuclear astrophysics is the theoretical description of a rapid neutron-capture nucleosynthesis process (the historical r-process) which is considered to be the origin of about half of the heavy element nuclides beyond Fe in our Solar System. This long-standing problem has been considered number three among: “*The 11 Greatest Unanswered Questions in Physics*” (Haseltine et al. 2002).

Since the seminal papers of Burbidge et al. (1957); Cameron (1957) and Coryell (1961), who identified the basic astrophysical and nuclear conditions for an r-process in explosive environments with high neutron density and temperature, r-process research has been quite diverse in terms of suggested stellar scenarios (for representative reviews, see e.g. (Cowan et al. 1991; Thielemann et al. 2011)). Still today, a robust production site for a full r-process with Solar-System-like abundances up to the actinide chronometers ^{232}Th and ^{238}U has yet to be determined.

To experimental and theoretical nuclear physicists and chemists, modeling the r-process has remained a particularly fascinating challenge over more than 50 years. Its detailed study in terms of isotopic and elemental abundances requires input of nuclear-structure data from the line of β -stability to the neutron drip line. Simple parameterized, but nevertheless informative studies of the r-process have been presented by many authors based on input of just a few nuclear properties, namely the nuclear mass (from which neutron separation energies S_n and β -decay Q_β values can easily be calculated), the β -decay half-lives $T_{1/2}$ and the probabilities of β -delayed neutron emission P_n . More elaborate, dynamical studies require additional nuclear quantities, such as reaction

rates, fission barriers, fission-fragment yields and temperature dependencies of various parameters.

A considerable leap forward in the basic understanding of the required astrophysical conditions at the time of r-process freeze-out for neutron densities occurred about two decades ago (Kratz et al. 1993). At that time, nuclear data from earlier versions of our global, unified, microscopic nuclear-structure models for nuclear masses (FRDM(1992)), published in Möller et al. (1995) and β -decay (the deformed quasi-particle random-phase (QRPA) model for Gamow-Teller (GT) β -decay in the form of Möller et al. (1997), based on the original work by Krumlinde & Möller (1984)), together with the first few experimental data on r-process isotopes at $N = 50$ and $N = 82$ (see, e.g. Kratz et al. (1988)), were used for the first time in such calculations. Among the main results of this investigation was a more detailed understanding of the impact of shell structure far from stability, considerably beyond the early recognition of the importance of spherical neutron shell closures. For example, the occurrence of the big r-abundance trough in the transitional mass region $115 \leq A \leq 125$ was explained, for the first time the astrophysical consequences of a significant weakening of the $N = 82$ shell strength below doubly magic ^{132}Sn were predicted, and evidence for a dramatic lowering of the neutron- $g_{7/2}$ orbital was found (Kratz et al. 1993). Motivated by these findings we initiated a large series of nuclear-structure experiments at CERN/ISOLDE, which in the following years led to the identification of more than 20 new r-process-relevant isotopes in the $A \simeq 130$ mass region (see, e.g. Kautzsch et al. (2000); Hannawald et al. (2000); Dillmann et al. (2002, 2003); Shergur et al. (2002, 2005); Kratz et al. (2005); Arndt et al. (2011)), as well as the

collection of all relevant neutron and proton-particle and hole states around ^{132}Sn (see, e.g. Kratz et al. (2000)), including first evidence of the most difficult to identify $p_{1/2}$ and $p_{3/2}$ proton-hole states and their spin-orbit splitting in $N = 82$ ^{131}In (Arndt et al. 2009).

Also concerning the FRDM(1992) mass model, over the next several years, step by step improvements of the FRDM mass model have been implemented but only now finalized. Similarly, numerous enhancements have been added to the initial QRPA model, and an extensive discussion of the improved version has been published in Möller et al. (2003). We therefore have available new consistent sets of the most essential nuclear-physics data.

With respect to our r-process parameter studies, since 1993 the site-independent waiting-point approach was steadily refined over the subsequent decade and applied to various comparisons with classical and new astronomical observations (Cowan et al. 1999; Pfeiffer et al. 2001; Sneden et al. 2003; Kratz et al. 2007; Ott & Kratz 2008). Starting in the early new millennium, we have replaced the above approach with more realistic, site-dependent dynamical r-process calculations within the high-entropy wind (HEW) scenario of core-collapse supernovae (cc-SN). In this effort, the basic Basel model (Freiburghaus et al. 1999) has been extended and improved by Farouqi et al. (2005, 2009a, 2010), and is still being used by our group today. With this HEW model, several important parameter studies have been performed to explain various recent astronomical observations (see, e.g. Farouqi et al. (2009a, 2010); Roederer et al. (2009, 2010); Hansen et al. (2012)).

The aim of the present Article is to present dynamical nucleosynthesis calculations within the HEW scenario, with the use of a new, improved global set of nuclear-physics quantities based on the new mass model FRDM(2012) and deformed QRPA calculations of β -decay properties. We point out the major improvements in the overall reproduction of the S.S. isotopic r-abundance residuals (Lodders et al. 2009; Bisterzo et al. 2011), as well as some remaining local deficiencies, which are smaller than previously but can provide important insights. Our FRDM and QRPA model combination provides not only masses and half-lives for the r-process calculation itself but many other associated quantities, e.g. deformations. This in-depth information permits us to propose more definite conclusions about nuclear structure far from stability through detailed comparisons between calculated results and observations.

2. MODELS

2.1. The FRDM(2012) mass model

The first Los Alamos macroscopic-microscopic mass model, based on the modern folded-Yukawa single-particle potential with a globally optimized Möller et al. (1974) spin-orbit force was published in 1981 Möller & Nix (1981). An enhanced version, the finite-range droplet model, FRDM(1992), which also extended the region considered to include all nuclei between the proton and neutron drip lines, was published in 1995 (Möller et al. 1995). This version now has been further refined during the first 13 years of the new millennium in 6 steps, 5 of which are enumerated in Figure 1 in Möller et al. (2012). The final improvement,

leading to the new mass table FRDM(2012) is a more accurate calculation of zero-point energies which further decreases the model error by 0.01 MeV, and removes well-known discontinuities in S_{1n} . With the completion of these steps, we froze the model on 09/06/2012, and are working on submitting FRDM(2012) to ATOMIC DATA AND NUCLEAR DATA TABLES. The accuracy with respect to AME2003 is 0.56 MeV, but higher, 0.42 MeV, above $N \simeq 50$, the region relevant for the r-process.

It is important to recall again that in our macroscopic-microscopic approach a mass table is not only a set of nuclear masses (or total binding energies), but just one result of a larger theoretical and computational effort that also provides ground-state (g.s.) shapes, g.s. spins and parities, gross β -decay properties, decay spectra in terms of allowed GT transition log ft values to daughter states, and many other related quantities. There is also an associated single-particle-model computer code so that one can with straightforward development obtain matrix elements of other operators of interest, for example electric quadrupole moments and charge radii. For our current r-process studies, we have calculated new tables of $T_{1/2}$ and $P_{\nu n}$ based on Q -values and ground-state deformations from the new mass table. Deformations determined from detailed calculations of multi-dimensional potential-energy surfaces are essential for obtaining realistic β -decay transition spectra from the parent ground states as well as from excited states of possible β -isomers. Our work here is unique in the sense that it obtains all nuclear data needed (ground-state deformations, masses, half-lives and delayed-neutron emission probabilities) from a single, consistent, global model framework, which has been favorably compared to a substantial body of experimental data. Furthermore, we obtain quantities not just for even-even nuclides, as do for example Stoitsov et al. (2003); Delaroche et al. (2010); Niu et al. (2013) but also for odd-even and odd-odd nuclides, with level structure and the associated decay schemes based on realistic intrinsic deformations. This allows us to interpret the inevitable remaining differences between calculations and observational data in terms of physics not yet included in the model, or, possibly as issues with the experimental evaluations. Excellent examples of previous such developments are, for example, 1) in theory: large differences between masses calculated in the original 1981 mass model Möller & Nix (1981) and measured masses in the Ra region were removed by inclusion of octupole-type shape distortions in the model deformation space Möller & Nix (1981); Möller et al. (2006), and 2) in experiment: masses that were in the AME1993 data base that deviated strongly from our calculations were removed or reevaluated in the AME2003 data base, see Möller (2008) for a discussion.

We show in Figure 1 the differences between calculated and experimental masses from the 2003 mass evaluation of Audi et al. (2003) in our current FRDM(2012) and the previous FRDM(1992). At first sight, the new model may not seem significantly better than the old one, but this is a fallacy. The overall model error has been improved from $\sigma_{\text{th}} = 0.6314$ MeV to $\sigma_{\text{th}} = 0.5595$ MeV, that is by about 13%. Although the region below $N \simeq 66$, that is below neutrons mid-shell between $N = 50$ and $N = 82$ shows larger correlated, fluctuating deviations near closed shells and in the transitional re-

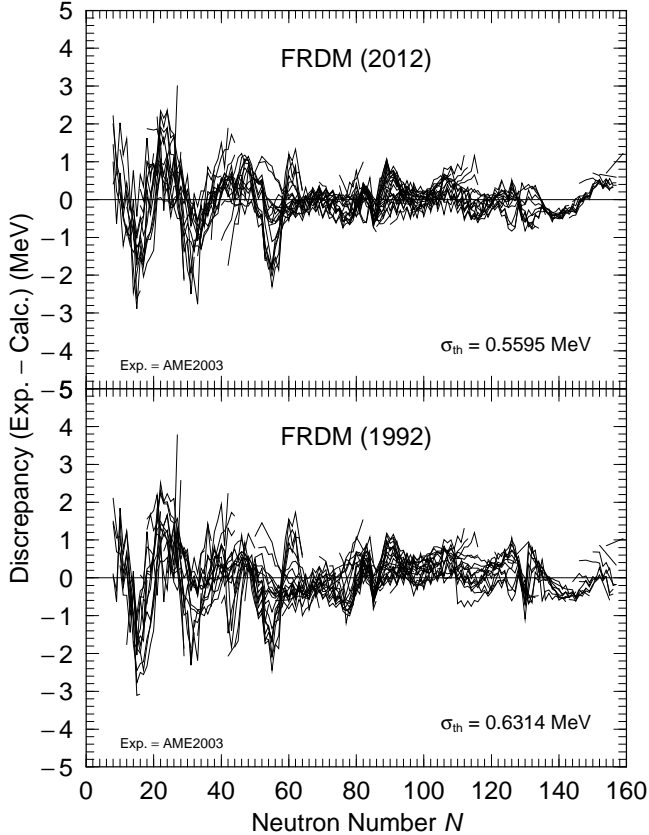


Figure 1. The FRDM(1992) and the FRDM(2012) both compared to the same experimental data set AME2003.

gion around the sub-shell $N = 56$ compared to the heavier region, these deviations have minimal impact on our HEW r-process calculations. In the heavier region above, the accuracy is significantly improved with $\sigma_{th} = 0.36$ MeV. Detailed areas of improvements are: 1) the bump of negative deviations just beyond $N = 40$ has largely disappeared, 2) the negative bump at $N \simeq 76$ is reduced, due to the incorporation of axial asymmetry, 3) the large-amplitude fluctuations in the deviations present in the vicinity of $N = 82$ are much reduced, especially below the magic number, and, as a final observation 4) the large fluctuations near $N = 126$ have almost disappeared.

Moreover, other very short-range fluctuations in the deviations are reduced. These fluctuations give large errors in calculated mass derivatives, such as isobaric mass differences (Q_β), neutron separation energies (S_n) or Q_α values, since they are directly sensitive to the derivative of $M_{exp} - M_{calc}$. These drastically decreased in the $Z \simeq 50$, $N \simeq 82$ Sn and in the $Z \simeq 82$, $N \simeq 126$ Pb regions. For $N > 50$ and $S_{1n} < 5$ MeV the S_{1n} rms deviation is 0.341 MeV for FRDM(1992), 0.320 MeV for FRDM(2012), 0.443 MeV for HFB21 (Goriely et al. 2009) and 0.361 MeV for HFB24 (Goriely et al. 2010). However, the HFB models are not fully microscopic, because various phenomenological terms are added to the potential energy obtained as HFB solutions. Such terms are the Wigner term with several adjustable parameters, the HFB mass models are surely not microscopic self-consistent models, but rather macroscopic-microscopic just like ours. How the FRDM improvements “visibly”

impact the calculated HEW r-process abundances are discussed later in Section 3.

2.2. Prediction of $T_{1/2}$ and P_n values from FRDM - QRPA

Beta-decay half-lives $T_{1/2}$ and delayed-neutron emission probabilities P_n are among the easiest measurable gross β -decay quantities of neutron-rich nuclei far from stability. Apart from their longstanding importance for reactor applications, the two properties have also become important in interpreting nuclear-structure features far from stability and in explosive nucleosynthesis studies. Theoretically, both integral quantities are interrelated via their usual definition in terms of the so-called β -strength function [$S_\beta(E)$] (Duke et al. 1970; Kratz 1984). The half-life may yield information on the average β -feeding of a nucleus. However, since the transition rates to low-lying single-particle states are strongly enhanced by the phase-space factor $f \sim (Q_\beta - E^*)^5$, where E^* is the excitation energy of the daughter final states, $T_{1/2}$ is most sensitive to the low-energy region of the β -strength function. The β -delayed neutron-emission probability P_n is schematically given by the ratio of the integral β -intensity to states above S_{1n} to the total β -intensity. Again, because of the $(Q_\beta - E^*)^5$ dependence of the Fermi function, the P_n are mainly sensitive to the β -feeding to the energy region just above S_{1n} . However, taking together the two gross decay properties, $T_{1/2}$ and P_n , may provide some primary information about the nuclear structure determining the β -decay.

Since the first simple, phenomenological approach of the “Kratz-Herrmann Formula” Kratz & Herrmann (1973), with updated compilations by Pfeiffer et al. (2002); McCutchan et al. (2012), numerous theoretical models have been used to predict $T_{1/2}$ and P_n values of unknown exotic isotopes; however many of these calculations were limited to localized mass regions. For a detailed discussion of the significance and sophistication of such models, see, e.g. Möller et al. (2003). In the present study, we use again the FRDM-QRPA formalism as outlined in Möller et al. (2003), now based on the FRDM(2012) model. We again take into account allowed GT and ff transitions, and as previously introduce an empirical Gaussian spreading of the individual GT transition strengths above 2 MeV, with width roughly corresponding to the model mass accuracy.

In Figure 2 we compare measured β -decay half-lives with calculations based on our models for pure GT and GT+ff transitions, for nuclei throughout the periodic system. To address the reliability versus distance from stability, we present the ratio $T_{\beta,calc}/T_{\beta,exp}$ versus the quantity $T_{\beta,exp}$. As in our earlier work (Möller et al. 1997; Pfeiffer et al. 2002; Möller et al. 2003) we find that the relative deviation between calculated and measured half-lives decreases towards smaller measured $T_{\beta,exp}$, which means the error decreases with distance from stability. Furthermore, our half-life comparisons show that the mean deviation of the calculated from the experimental values are approximately zero. This indicates, that no “renormalization” of the calculated β -strength is necessary. The calculated half-lives agree with the 272 experimental values listed in NUBASE2012 with $T_{1/2} \leq 1$ s to within a factor of 2.68.

In Figure 3, we compare measured β -delayed neu-

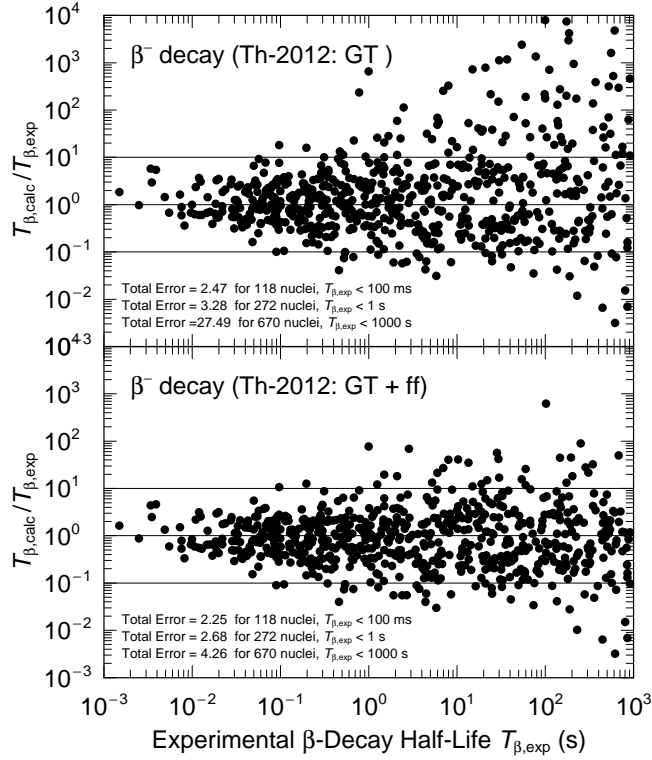


Figure 2. Ratio of calculated to experimental β -decay half-lives $T_{1/2}$ for nuclei from ^{16}O to the heaviest known ones. In the upper part, only the theoretical GT-strength is considered, whereas in the lower part GT+ff calculations are used for comparison. The respective total errors are given for three different half-life ranges, i.e. $T_{1/2} < 1000$ s, < 1 s and < 100 ms, where the last limit represents the usual range for r-process nuclei. For further details, see text and (Pfeiffer et al. 2002; Möller et al. 2003)

tron emission probabilities with the calculations based on our two models for nuclei in the fission-fragment region. Again, to address the reliability versus distance from stability we present the ratio $P_{n,\text{calc}}/P_{n,\text{exp}}$ versus the quantity $T_{\beta,\text{exp}}$. Although for the P_n quantity, we still have substantially fewer data than for the $T_{1/2}$ values, similar trends are observed when comparing to the predictions for pure GT-decay. When the ff strength is added we again find that the new calculation gives improved agreement with experimental data. The calculated P_n values agree with the NUBASE2012 values to within a factor 3.39 for the 188 nuclei, where we in this case compare to the full half-life range.

2.3. The HEW r-process model

The basic nucleosynthesis mechanisms for elements beyond Fe by slow (s-process) and rapid (r-process) captures of neutrons have been known for long time (Burbidge et al. 1957; Cameron 1957; Coryell 1961). However, the search for a robust r-process production site has proven difficult. Still today, all proposed scenarios not only face problems with astrophysical conditions, but also with the necessary nuclear-physics input for very neutron-rich isotopes. Among the various r-process sites suggested during the past decades, the most recent ones supposedly favored in the nucleosynthesis community, are neutron star mergers (NSM; see, e.g. (Korobkin et al. 2012; Goriely et al. 2013)) and mag-

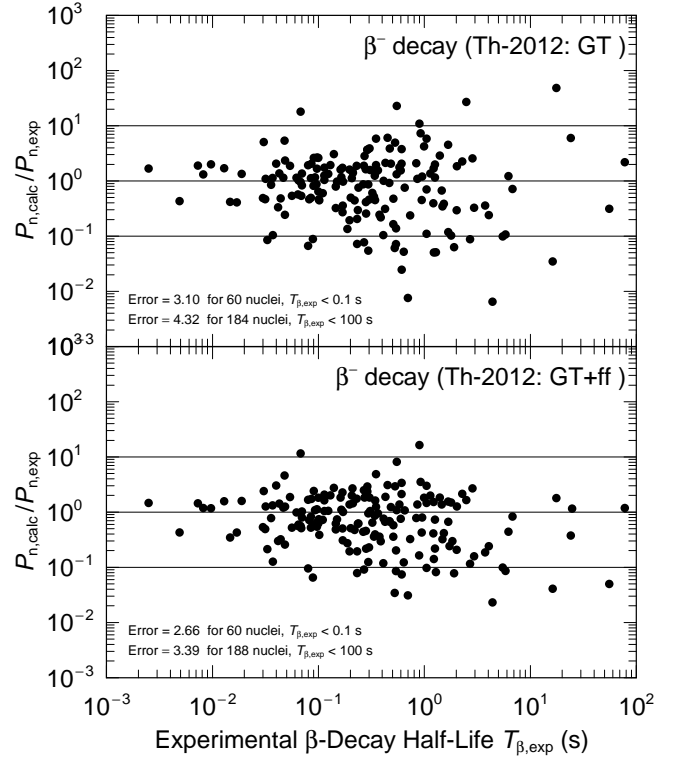


Figure 3. Ratio of calculated to experimental β -decay neutron-emission probabilities P_n . In the upper part only the theoretical GT-strength is considered, whereas in the lower part GT+ff calculations are used for comparison. The respective total errors are given for the whole ensemble of β -decay precursors, and for the limited number of r-process nuclei with $T_{1/2} < 100$ ms. For further details, see text and (Pfeiffer et al. 2002; Möller et al. 2003)

netorotationally driven SNe (see, e.g. (Winteler et al. 2012)). However, even these scenarios are not fully convincing. On the one hand, NSMs, apart from the still ongoing debates whether they can be responsible for the r-process observations in metal-poor halo stars in the early Universe, the resulting abundance patterns of the heavier elements differ from the S.S.-r one. This does not exclude the merger scenario; however, it seems unlikely that the NSM r-process represents the dominant origin of the “main” r-component with $A \geq 130$. On the other hand, magnetohydrodynamic SNe explosion models (still) require extremely high magnetic fields and strong rotation to produce bipolar jets with possible r-process matter ejecta. However, also this promising scenario has been questioned, e.g. Fryer & Young (2007) and by the recent 3D simulations of Moesta et al. (2014). Therefore, in our r-process parameter studies we prefer to use the neutrino-driven or high-entropy wind (HEW) of core-collapse SNe, which still is one of the best studied “classical” mechanisms (for representative publications over the last two decades see, e.g. (Woosley et al. 1994; Takahashi et al. 1994; Wanajo et al. 2001, 2006; Farouqi et al. 2009a,b, 2010)). However, until recently even the most sophisticated hydrodynamical models have predicted that the neutrino-driven wind is proton-rich (electron fraction $Y_e > 0.5$) during its entire life, thus actually precluding a rapid neutron-capture process (see, e.g. (Fischer et al. 2010; Roberts et al. 2010)). How-

ever, recent work on charged-current neutrino interaction rates (see, e.g. (Roberts et al. 2012; Martinez-Pinedo et al. 2012)) seems to revive the HEW scenario as a possible r-process site by predicting that Y_e can well reach neutron-rich conditions a few seconds after bounce, with minimal values of $Y_e \simeq 0.42$ but still with too low entropies of $S \leq 120$. When considering in addition active-sterile neutrino mixing, Wu et al. (2014) even predict Y_e values down to about 0.31. Under such $Y_e - S$ conditions, the production of the light trans-Fe elements from Sr up to about Cd would be possible. However, the heavier (REE and 3rd peak) elements observed in ultra-metal-poor halo stars (see, e.g. (Roederer et al. 2010)) would not (yet) be produced. Furthermore, it is admitted that there are still various model uncertainties about weak rates, nuclear symmetry energy, weak magnetism, inelastic processes, etc. (Fischer 2014). Also the versions of the equation of state (EOS) used in the above calculations do not seem to be the optimum choice, since they fail several tests related to symmetric nuclear matter, pure neutron matter and/or symmetry energy, and its derivatives (Dutra et al. 2014). Therefore, a final conclusion about the realistic $Y_e - S - V_{\text{exp}}$ parameter space of the cc-SN scenario can presumably not yet be drawn. Given the present model situation, and since the main goal of the present paper is to compare the results with the old and new FRDM & QRPA nuclear-physics input to r-process abundance calculations, to us it appears justified to use again our parameterized, dynamical HEW approach, based on the initial model of Freiburghaus et al. (1999), which assumes adiabatically expanding homogeneous mass zones with different values of the radiation entropy S (in k_B /baryon). The code used for the nucleosynthesis calculations (see Farouqi et al. (2010)) has been steadily improved, for example to implement experimental data as well as more reliable theoretical β -decay properties in certain “pathological” mass regions (see, e.g. Arndt et al. (2011)). Furthermore, a better algorithm has been developed for the tracking of the β -decaying nuclei back to stability with time-intervals small enough to consider very late recaptures of previously emitted β -delayed neutrons from longer-lived precursors, such as 55s ^{87}Br or 24s ^{137}I .

As has been outlined in detail in Farouqi et al. (2010), the overall wind ejecta represent a superposition of S components, where the main parameters Y_e , S and the expansion velocity V_{exp} (in km/s) are correlated via the “r-process strength formula” $Y_n/Y_r \propto V_{\text{exp}} \times (S/Y_e)^3$. Following our traditional attempt to find a possible explanation of the S.S. isotopic abundance residuals ($N_{r,\odot} \simeq N_{\odot} - N_{s,\odot}$; Lodders et al. (2009); Bisterzo et al. (2011)), eventually from a weighted superposition of several HEW conditions and using for the first time the new FRDM-QRPA nuclear-physics input, we have investigated the whole astrophysics parameter space as functions of electron abundance ($0.40 \leq Y_e \leq 0.499$), expansion velocity ($2000\text{km/s} \leq V_{\text{exp}} \leq 30\,000\text{km/s}$).

3. REPRODUCTION OF THE S.S. R-PROCESS ABUNDANCES

In this Article, we present first results of our HEW study based on the new FRDM(2012) and QRPA(2012) nuclear-physics input as outlined in subsections 2.1 and 2.2, and our “standard” choice of the astrophysical pa-

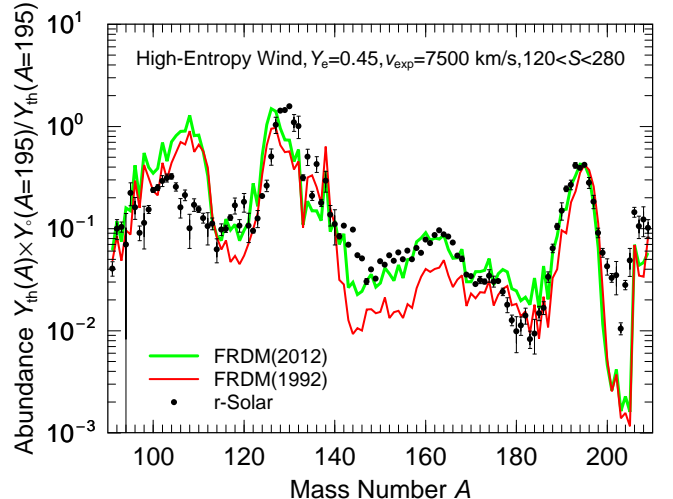


Figure 4. Solar r-process abundances compared to calculations based on two nuclear-structure data bases: our previous FRDM(1992) and the new FRDM(2012). Both calculated distributions are normalized to the $N_{r,\odot}$ value of ^{195}Pt at the maximum of the $A \simeq 195$ peak.

rameters of $Y_e = 0.45$, $V_{\text{exp}} = 7500$ km/s and $20 \leq S \leq 280$ k_B /baryon. This simulates “hybrid” r-process conditions with freezeout-temperatures (when $Y_n/Y_r \leq 1$) for free neutrons of $T_9(\text{freeze}) \simeq 0.7$ for the $A \simeq 130$ abundance peak. For this nuclear and astrophysics input, we show in Figure 4 the integrated r-abundances ($N_{r,\text{calc}}$) for our new (2012) calculations together with the $N_{r,\odot}$ values and our results based on the previous FRDM(1992) and QRPA(2003) nuclear-physics input, both curves normalized to the $N_{r,\odot}$ value of (98% “r-only”) ^{195}Pt . Both $N_{r,\text{calc}}$ distributions represent results of the integration over the total mass region with a consistent weighting of equal-sized ejected HEW elements with equidistant entropies as outlined in Farouqi et al. (2010). Hence, they are not composed of a superposition of independently fine-tuned fits of local mass regions, which may in each case yield better agreement with the $N_{r,\odot}$ pattern, as for example shown by Arndt et al. (2011) for the $A \simeq 130$ r-peak or by Mumpower et al. (2012) for the REE region alone. Therefore, at first sight the new overall $N_{r,\text{calc}}$ distribution may not seem significantly better than the old one, but this impression is deceiving as will be discussed in the following.

First, let us motivate why in Figure 4 we only show the r-abundance pattern for the entropy range $S \geq 120$, i.e. the region of the HEW components of the “weak” and “main” neutron-capture components. As is well known, in the HEW scenario a significant overproduction of the mass region below $A \simeq 110$ seems to be unavoidable (see, e.g. Woosley et al. (1994); Freiburghaus et al. (1999); Farouqi et al. (2009a, 2010)). This result has commonly been referred to as a model deficiency due to the α -rich freezeout component at low S , which – according to the definition given in Farouqi et al. (2009a) – concerns the “charged-particle” and part of the “weak” neutron-capture components with the elements between Sr and Ag. In Farouqi et al. (2010) it has been speculated that one could avoid this discrepancy by considering HEW ejecta as a mixture of correlated S and Y_e

components. However, in our present study we are again unable to verify this assumption. Hence, even with the new nuclear-physics (FRDM(2012)–QRPA(2012)) input the local overabundance in the $100 \leq A \leq 110$ mass region persists. Moreover, as is partly indicated in Figure 4, in this mass region there is also no improvement of the abundance fit relative to the earlier FRDM(1992)–QRPA(2003) input.

However, in the heavier $A \simeq 120$ mass region where in the past in practically all r-process calculations with the FRDM(1992) masses, the large abundance trough occurred (see, e.g. Kratz et al. (1993); Wanajo et al. (2004); Farouqi et al. (2010); Winteler et al. (2012); Nishimura et al. (2012)), we now see that with the new FRDM(2012) masses this discrepancy has practically disappeared. As has in principle already been discussed long time ago (see, e.g. Kratz et al. (1993); Chen et al. (1995); Pfeiffer et al. (1997)), this trough effect is due to subtle details in the predicted behavior of the decreasing absolute magnitude of the slope $dS_{1n}(N)/d2N$ for odd N of the r-process isotopes of Zr to Tc between the strongly deformed $N = 66$ neutron mid-shell and the shape-transition region towards the next major spherical shell closure at $N = 82$. Taking, for example the isotopic chain of ^{40}Zr , with the FRDM(1992) model predictions the r-process “boulevard” with increasing neutron-density or S components was populated by isotopes up to odd- N $^{113}\text{Zr}_{73}$ with the predicted lowest $S_{1n} = 1.36$ MeV and an unusually strong prolate quadrupole deformation of $\epsilon_2 = 0.36$. Thereafter, instead of an expected further decrease of the S_{1n} values, an increase of S_{1n} of 0.78 MeV occurred in FRDM(1992) between $N = 73$ and $N = 75$, and S_{1n} remains large until the $N = 82$ magic shell. The consequence of this behavior has been that the Zr r-abundances pile up in the lower-mass even- N “waiting-points” up to $^{112}\text{Zr}_{72}$; and then the r-process directly “jumps” over 10 mass units to the classical neutron-magic waiting-point $^{122}\text{Zr}_{82}$. With the similar behavior of the $dS_{1n}(N)/d2N$ slopes of the neighboring elements in this mass region, in the extreme case of an instantaneous freezeout no r-progenitor isotope is produced in the initial r-process “boulevard” between $A = 112$ and the $N = 82$ isotones of Zr to Tc (see, e.g. Figure 4 in Chen et al. 1995). The resulting deep trough occurring under these simplified conditions cannot be completely filled up by late non-equilibrium captures of free neutrons and/or the recapture of previously emitted β -delayed neutrons during a more realistic treatment of the freezeout phase, as one can see, for example from Figure 24 in Farouqi et al. (2010), and also from Figure 4 in this Article.

In the FRDM(2012), however, the description of this shape-transition region is improved. Taking again the Zr isotopes as an example, the r-process also runs up to $^{113}\text{Zr}_{73}$ with its lowest, but now somewhat higher $S_{1n} = 1.74$ MeV and a slightly lower – but probably still too high – deformation of $\epsilon_2 = 0.33$ (cf. Pereira et al. (2009)). Thereafter, again a local increase of the S_{1n} occurs, but less pronounced than in FRDM(1992). Thus, in the Zr chain the next populated r-process progenitor is $^{119}\text{Zr}_{79}$. With the similar behavior of the S_{1n} slopes of the neighboring elements, in the FRDM(2012) several r-progenitor isotopes are populating the r-process “boulevard” in the $A \simeq 120$ mass region. As seen in Figure 4,

this population together with a realistic dynamical treatment of the full freezeout phase now removes the earlier r-abundance trough.

While the occurrence of this trough below the $A \simeq 130$, $N_{r,\odot}$ peak in earlier approaches could be considered as a local “eyesore” in the calculated r-abundance distribution, its nuclear-structure correlation to the $N = 82$ shell closure is of considerable importance for the r-process production of the heavy elements. It has been shown that the neutron shell strength below doubly magic ^{132}Sn strongly influences the formation of this peak, and acts as an important bottle-neck for the further r-process matter flow via the rare-earth-element (REE) pygmy-peak region and the next major peak at $A \simeq 195$ to the actinide r-chronometer region.

In Figure 4 we show the $N_{r,\text{calc}}$ pattern of the $A \simeq 130$ r-peak for the above “standard” astrophysics parameter combination, again with both the old and new nuclear-physics input. It is immediately evident that with the chosen single Y_e component, no significant “visible” improvement of the $N_{r,\odot}$ peak is obtained when compared to the fit with the older FRDM(1992) nuclear-data input. The maximum of the peak is already reached at $A = 126$, instead of $A = 130$, and the right wing of the peak is underproduced. Apart from this remaining deficiency, however, the change of the overall trend of the S_{1n} values in the $N = 82$ region with the new FRDM(2012), and in particular the trend of a decreasing shell-gap below doubly-magic $^{132}_{50}\text{Sn}_{82}$, defined as the difference of the S_{2n} values for $N = 82$ and $N = 84$, has the welcome effect of reducing the earlier overly strong bottle-neck behavior of the $N = 82$ shell. While with FRDM(1992) the shell gap below $Z = 50$ was predicted to further increase with decreasing proton number down to $Z = 40$, with the new FRDM(2012) the trend is inverted, and is now similar to the predictions from the recent HFB versions and the so-called “quenched” mass formulas, such as ETFSI-Q (Pearson et al. 1996).

As we have shown already in Pfeiffer et al. (2001), in fact the correlated effects of nuclear masses (S_n values) and β -decay properties ($T_{1/2}$) have important consequences for the further time behavior and the amounts of heavier r-abundances in the matter flow out of the $A \simeq 130$ peak to the REE region and beyond. While the time interval needed from the r-seed composition of the α -rich freezeout to reach the maximum of the 2nd r-peak still is about the same (for $20 \leq S \leq 190$, $\tau_r \simeq 160$ ms) for the old and new nuclear-physics input, the time to overcome the peak bottle-neck within the S range $190 \leq S \leq 210$ is with $\tau_r \simeq 160$ ms for FRDM(1992) already significantly longer than that for FRDM(2012) with only $\tau_r \simeq 95$ s. This time difference then continues for the formation of the REE and the $A \simeq 195$ peaks, resulting in total r-process durations (for the whole S -ranges of $20 \leq S \leq 280$) of $\tau_{r,\text{tot}} \simeq 680$ ms in the past, whereas with FRDM(2012) a “speeding-up” of the r-process is obtained with a $\tau_{r,\text{tot}} \simeq 535$ ms.

With respect to the exact shape and position of the $A \simeq 130$ peak, we can furthermore check why we do not meet the maximum of the peak exactly at $A = 130$. A closer look at the S_{1n} values of the $N = 83$ isotopes below $Z = 50$ for FRDM(2012) shows the expected (and for the r-process “favored”) smooth decrease by about 1.47

MeV between $^{133}_{50}\text{Sn}$ and $^{128}_{45}\text{Rh}$. However, when continuing further down in Z to $N = 83$ ^{127}Ru and ^{126}Tc , in FRDM(2012) a sudden drop in S_{1n} by 0.55 MeV occurs, followed by even negative S_{1n} values for ^{125}Mo to ^{123}Zr , which is not predicted in “quenched” mass formulas. Quite obviously, it is this local S_{1n} behavior that causes the largest bottle-neck for the r-process at these mass numbers, resulting in the observed maximum of the $N_{r,\text{calc}}$ peak already at $A = 126$ with the FRDM(2012) masses and the above HEW conditions. We know from earlier r-process studies with the “quenched” mass model ETFSI-Q that relative to our standard conditions of a “hybrid” r-process variant (with $T_{9,\text{freeze}} = 0.8$ and a time duration until freezeout of $\tau_r = 130$ ms) for the condition of a “hot” r-process variant (with $T_{9,\text{freeze}} = 1.2$ and a time duration until freezeout of $\tau_r = 560$ ms) the maximum of the peak can be shifted from $A = 128$ to $A = 130$ and even slightly beyond. Therefore, we have also checked the outcome of our HEW calculations with the new FRDM(2012), and have obtained similar results. We thus conclude that within our HEW model the correct shape and position of the $A \simeq 130$ r-abundance peak can only be reproduced by a weighted superposition of different Y_e -components.

The next subject of our discussion of the $N_{r,\text{calc}}$ pattern is the pygmy-peak region of the REE in between the two major r-peaks. As can be seen from Figure 4, considerably improved agreement with $N_{r,\odot}$ is achieved with the new FRDM(2012) input. With the FRDM(1992) masses, the whole REE region of $140 \leq A \leq 180$ is underestimated by a mean factor of 1.67, whereas with the new nuclear input the overall agreement in shape and abundance magnitude is excellent, with a mean factor of only 0.97. The reason for this improvement clearly lies in the reduced bottle-neck behavior of the $A \simeq 130$ major r-process peak, which obviously has enabled a higher r-matter transfer to the REE mass region within the respective S-range of $210 \leq S \leq 250$. This shows that earlier speculations that significant feeding from fission cycling would be necessary to properly fill up the REE region can be excluded. This assumption was introduced to “repair” a clear nuclear-model deficiency by addition of fission-material originating from unrealistically high S components ($S \geq 400$) with unusually high weights of r-progenitor isotopes in the heavy actinide region. Within the HEW scenario combined with the FRDM(2012)-QRPA nuclear-structure data the REE peak is well reproduced without invoking fission recycling.

Both our $N_{r,\text{calc}}$ distribution for FRDM(1992) and FRDM(2012) have been normalized to the S.S. r-abundance of ^{195}Pt . With this normalization the shape and position of the 3rd r-process peak are well reproduced, with a slight improvement of the rising wing of the peak with FRDM(2012). This shows that with FRDM(2012) the shape-transition region before the peak and the $N = 126$ shell strength are described correctly.

In contrast, the shape-transition region above $N = 126$ may still be imperfect, as is evident from the deep r-abundance trough in the $199 \leq A \leq 205$ region. Just as in the $A \simeq 120$ region, the S_{1n} slopes of the specific elements of $_{68}\text{Er}$ to $_{70}\text{Yb}$ show a “bump” behavior beyond $A \simeq 198$, thus precluding significant initial and

final r-abundances below the Pb region. In addition to the S_{1n} effect, probably also the onset of collectivity beyond the $N = 126$ shell closure seems to set in somewhat too early. A possible indication for this speculation is that a HEW calculation with FRDM(2012) masses and spherical β -decay properties indicates a significantly better reproduction of the $A \simeq 204$ trough region.

As the last point of our comparison of how the $N_{r,\text{calc}}$ agrees with the $N_{r,\odot}$ pattern, we point out that the predicted underabundances for the Pb and Bi isotopes shown in Figure 4 occur because here the important abundance fraction from the α - backdecays from the actinides has not (yet) been added.

As a brief summary of our Article we find that the new nuclear-structure data base has removed some much-studied differences between calculated and observed S.S. abundances without resorting to arbitrary changes of relevant sections in the calculated data bases as has been the practice in many previous and present studies. With our use of a fully consistent model framework, namely the FRDM(2012) and QRPA(2012) combination as input for r-process calculations, we again demonstrate that, coupled with detailed comparisons with astronomical and cosmochemical observations, this approach is a valuable tool for learning about both nuclear structure far from stability and the required astrophysical conditions for a full r-process.

First, we would like to acknowledge the constructive criticism of the anonymous referee, who greatly helped to improve our paper. Furthermore, we thank Jirina Stone, Tobias Fischer, Matthias Hempel and Mounib El Eid for fruitful discussions. PM carried out this work under the auspices of the National Nuclear Security Administration of the U. S. Department of Energy at Los Alamos National Laboratory under Contract No. DE-AC52-06NA25396.

REFERENCES

- Arndt, O., et al. 2009, *Acta Physica Polonica B*, 40, 437
- Arndt, O., et al. 2011, *Phys. Rev. C*, 84, 061307 (R)
- G. Audi, G., Wapstra, A.H., & Thibault, C. 2003, *Nucl. Phys. A* 729, 337
- Bisterzo, S., et al. 2011, *MNRAS*, 418, 284.
- Burbidge, E.M., et al. 1957, *Rev. Mod. Phys.*, 29, 547
- Cameron, A. G. W. 1957, *PASP*, 69, 201
- Chen, B., et al. 1995 *Phys. Lett. B*, 355, 37
- Coryell, C.D. 1961, *J. Chem. Education*, 38, No.2, 67
- Cowan, J.J., Thielemann, F.-K., & Truran, J.W. 1991, *Phys. Rep.*, 208, 267
- Cowan, J.J., et al. 1999, *ApJ*, 521, 194
- Delaroche, J.-P., et al. 2010, *Phys. Rev. C* 81 014303
- Dillmann, I., et al. 2002, *Eur. Phys. J A*, 13, 281.
- Dillmann, I., et al. 2003, *Phys. Rev. Lett.*, 91,162503
- Duke, C.L., et al. 1970, *Nucl. Phys.*, A151609
- Dutra, M., et al. 2014, (Relativistic Mean-Field Hadronic Models under Nuclear Matter Constraints), to be published
- Farouqi, K., et al. 2005, *Nucl. Phys. A*, 758, 631c
- Farouqi, K., et al. 2009, *ApJ*, 694, L49
- Farouqi, K., Kratz, K.-L., & Pfeiffer, B. 2009, *PASA*, 26, 194.
- Farouqi, K., et al., 2010, *ApJ*, 712, 1359
- Fischer, T., et al. 2010, *A&A*, 517, 80
- Fischer, T. 2014; lecture given at the 11th Russbach School on Nuclear Astrophysics; (<http://russbachwks2014.scienceconf.org>)
- Freiburghaus, C., et al. 1999, *ApJ*, 515, 381 & 516, 381
- Fryer, C.L. & Young, P.A. 2007, *ApJ*, 659, 1438

- Goriely, S., Chamel, N., & Pearson, J.M. 2009, Phys. Rev. Lett., 102, 152503
- Goriely, S., Chamel, N., & Pearson, J.M. 2010, Phys. Rev. C82, 035804
- Goriely, S., et al. 2013, Phys. Rev. Lett., 111, 242502
- Hannawald, M., et al. 2000, Phys. Rev. C, 62, 054301
- Hansen, C. J., et al. 2012, A&A, 545, A31
- Haseltine E. 2002, Discover Magazine, Vol. 23, No. 2
- Kautzsch, T., et al. 2000, Eur. Phys. A, 9, 201
- Korobkin, O., et al. 2012, Mon. Not. R. Astron. Soc., 426, 1940
- Kratz, K.-L., & Herrmann, G. 1973, Z. Phys., 263, 435
- Kratz, K.-L. 1984, Nucl. Phys., A417, 447
- Kratz, K.-L., et al., 1988, J. Phys. G: Nucl. Phys., 14, 331
- Kratz, K.-L., et al., 1993, ApJ, 403, 216
- Kratz, K.-L., et al., 2000, Hyperfine Interactions, 129, 185
- Kratz, K.-L., et al. 2005, Eur. Phys. J a, 25, s01, 633
- Kratz, K.-L., et al. 2007, ApJ, 662, 39
- Krumlinde, J., & Möller, P. 1984, Nucl. Phys. A, 417, 419
- Lodders, K., Palme, H., & Gail, H.-P., Landolt-Börnstein, 2009, New Series VI/4B, 4.4.
- Martinez-Pinedo, G., et al. 2012, Phys. Rev. Lett., 109, 251104
- McCutchan, E.A., et al. 2012, Phys. Rev. C, 86, 041305(R)
- Möller, P., Nilsson, S. G., & Nix, J. R. 1974, Nucl. Phys. A, 229, 292
- Möller, P., & Nix, J. R. 1981, Nucl. Phys. A 361, 117 & Möller, P., & Nix, J. R. 1981, ADNDT 26, 165
- Möller, P., et al., 1995, ADNDT 59, 185
- Möller, P., Nix, J. R., & Kratz, K.-L. 1997 ADNDT 66, 131
- Möller, P., Pfeiffer, B., & Kratz, K.-L. 2003, Phys. Rev. C, 67, 055802.
- Möller, P., et. al., 2006, Phys. Rev. Lett., 97, 162502
- Möller, P., et al., 2008, Proc. Int. Conf. on Nuclear Data and Technology, EDP Sciences, p. 69, ISBN 978-2-7598-0090-2)
- Möller, P., et al., 2012, Phys. Rev. Lett., 108, 05250
- Moesta, P., et al. 2014, ApJ, 785, L29
- Mumpower, M.R., McLaughlin, G.C., & Surman, R. 2012, ApJ, 752, 117
- Nishimura, N., et al., 2012, Phys. Rev. C, 85, 048801
- Niu, Z.M., et al., 2013, Phys. Lett. B, 723, 172
- Ott, U., & Kratz, K.-L. 2008, New. Astron. Rev., 52, 396.
- Pearson, J. M., Nayak, R. C., & Goriely, S. 1996, Phys. Lett. B, 387, 455.
- Pereira, J., et al. 2009, Phys. Rev. C79, 035806
- Pfeiffer, B., Kratz, K.-L., & Thielemann, F.-K. 1997 Z. Phys. 357, 235
- Pfeiffer, B., et al. 2001, Nucl. Phys. A, 693, 282
- Pfeiffer, B., Kratz, K.-L., & Möller, P. 2002, Progr. Nucl. Energy, 41, 39
- Roberts, L. F., Woosley, S. E., & Hoffman, R. D. 2010, ApJ, 722, 954
- Roberts, L. F., Reddy, S., & Shen, G. 2012, Phys. Rev. C, 86, 065803
- Roederer, I.U., et al. 2009, ApJ, 698, 1963
- Roederer, I.U., et al. 2010, ApJ, 724, 975
- Shergur, J., et al. 2002, Phys. Rev. C, 65, 03413
- Shergur, J., et al. 2005, Phys. Rev. c, 71, 064321
- Snedden, C., et al. 2003, ApJ, 591, 936
- Stoitsov, M.V., et al. 2003, Phys. Rev. C68, 054312
- Takahashi, K., Witt, J. & Janka, H.-T. 1994, A&A, 286, 857
- Thielemann, F.-K., et al. 2011, Prog. Part. Nucl. Phys., 66, 346
- Wanajo, S., et al. 2001, ApJ, 554, 578
- Wanajo, S., Goriely, S., Samyn M., & Itoh, N. 2004, ApJ, 606, 1057
- Wanajo, S., et al. 2006, ApJ, 636, 842
- Winteler, C., et al. 2012, ApJ, 750, L22
- Woosley, S.E., et al. 1994, ApJ, 433, 229
- Wu, M.-R., et al. 2014, Phys. Rev., D89, 061303(R)